Scientific Research Publishing

Journal of Biosciences and Medicines, 2026, 14(2), 138-148
https://www.scirp.org/journal/jbm
ISSN Online: 2327-509X
ISSN Print: 2327-5081

The Effects of Cyclic Stretch-Induced Cytoskeletal Reinforcement and Cell Alignment on the Cellular Wound Healing Processes

Kazuki Ikeda, Kazuaki Nagayama

Micro-Nano Biomechanics Laboratory, Department of Mechanical Systems Engineering, Ibaraki University, Ibaraki, Japan
Email: kazuaki.nagayama.bio@vc.ibaraki.ac.jp

How to cite this paper: Ikeda, K. and Nagayama, K. (2026) The Effects of Cyclic Stretch-Induced Cytoskeletal Reinforcement and Cell Alignment on the Cellular Wound Healing Processes. *Journal of Biosciences and Medicines*, **14**, 138-148.
https://doi.org/10.4236/jbm.2026.142012

Received: January 4, 2026
Accepted: February 2, 2026
Published: February 5, 2026

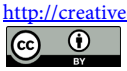

Abstract

When biological skin tissue is damaged, the surrounding fibroblasts migrate to the wound to seal the damaged area and promote healing. In the fields of medicine and pharmacology, efforts have been vigorously pursued to understand the biochemical signaling pathways involved in wound healing and to develop wound healing promoters utilizing endogenous factors. In recent years, there has been an increased focus on the effects of mechanical stimuli on cells. Specifically, researchers have discovered that applying cyclic stretch stimulation to cells causes them to align in a specific direction, strengthening the structure of the actin cytoskeleton within the cells. Understanding how the physical environment and mechanical stimuli influence cellular migration during wound healing is also critically important for developing artificial tissues with high wound-healing and regenerative capabilities. Therefore, this study used cultured skin fibroblasts to prepare three groups of cell tissues: control cells with random orientation (CON), control cells with natural orientation (CON-OR), and cells with remarkable orientation induced by cyclic stretch stimulation (CSS-OR). These cell tissue groups were wounded using a pulsed laser, and cell migration during wound healing was observed using live-cell imaging. To analyze individual cell migration, cell nuclei were fluorescently visualized, and cell migration trajectories and speeds were quantified. The wound healing rate of the CON-OR group was faster than that of the CON group, suggesting that the cells migrate preferentially in alignment. In contrast, wound repair migration was suppressed in the CSS-OR group, even though the cells were oriented toward sealing the wound. Cyclic stretch stimulation markedly induced cell reorientation; however, it may have strengthened cell-cell and cell-substrate adhesions by significantly reinforcing the actin cytoskeleton, thereby suppressing the migration of individual cells immediately after wound formation.

Keywords

Cell Biomechanics, Mechanobiology, Cell Migration, Laser Ablation

1. Introduction

When biological tissues such as skin or muscle are damaged, the cells in those tissues promote healing by activating wound repair mechanisms that seal the damaged area [1]. To understand these mechanisms and develop methods to enhance tissue repair, extensive research has been conducted in medicine and pharmacology. For instance, fibroblast growth factor (FGF) and epidermal growth factor (EGF), which mediate intercellular communication during wound healing, play crucial roles in tissue repair by promoting cell proliferation, migration, and inhibiting cell death. Healing promoters utilizing these growth factors have been developed and are partly used clinically as medical products. Additionally, "scaffold therapy" is a well-known method for promoting tissue repair. This therapy involves implanting a scaffold—a substrate that serves as a foundation for cell proliferation and invasion—into the damaged site to facilitate tissue regeneration. Scaffolds can be made from bio-derived collagen or bioabsorbable poly (glycolic acid) nanofibers. Studies on optimizing scaffold surface topography have shown that triangular microgroove patterns can significantly increase cell migration toward the damaged site [2].

As described above, the wound-healing movement of cells is primarily controlled by the actin cytoskeleton. It is linked to focal adhesions that contain the adhesion molecule integrin, as well as mechanoreceptors such as vinculin and talin. The actin cytoskeleton adheres to the extracellular matrix via focal adhesions, supporting cell structure and controlling cell migration [3] [4]. Recently, research has been conducted to promote wound healing by utilizing cellular responses to mechanical stimuli. In particular, mechanical stretch stimulation has been reported to affect cellular wound healing processes. A sustained, unidirectional stretch facilitated wound healing in bovine aortic endothelial cells, whereas a biaxial, cyclic stretch significantly inhibited wound repair in alveolar cell monolayers via actin disruption and a reduction in the colocalization of actin and vinculin [5] [6]. Our previous research showed that applying uniaxial cyclic stretch stimulation parallel to the wound direction significantly enhances cell motility at the wound leading edge, promoting wound closure [7]. However, previous studies have used continuous mechanical stretch stimulation throughout the cellular wound healing process. Consequently, it was unclear whether the cells' wound-healing capacity would be maintained after ceasing stimulation and returning them to a static condition. This is a critically important point for the application of scaffold therapy as an artificial tissue.

Therefore, in this study, we investigated migration behavior of skin fibroblasts

after wounding, using three cell tissue groups: the control cells with random orientation (CON), the control cells with natural orientation (CON-OR), and cells with remarkable orientation induced by cyclic stretch stimulation (CSS-OR). We then examined how the cytoskeletal structures of individual cells, cell-cell adhesion, and cell-matrix adhesion influence the wound healing behavior of cellular tissues.

2. Materials and Methods

2.1. Cell Culture

The telomerase-immortalized human foreskin BJ1 fibroblasts. The BJ1 fibroblasts were kindly provided by Dr. Nakamura A., Ibaraki University (Japan). The cells were cultured in Dulbecco's Modified Eagle Medium (DMEM, Invitrogen, USA) supplemented with 10% Fetal Bovine Serum (JRH Bioscience, USA), 100 U/mL Penicillin, and 100 μg/mL Streptomycin (Sigma) at 37˚C in 5% CO_2 atmosphere. These BJ1 fibroblasts are an immortalized cell line that stably expresses the DNA repair protein 53BP1, which is labeled with red fluorescence within the nucleus [8]. In this study, fluorescence images of intranuclear 53BP1 were used to track cell migration during wound healing.

2.2. Application of Cyclic Stretch

Silicone rubber membranes made with poly(dimethylsiloxane) (PDMS; SYLGARD 184, Dow-Corning) were used as an elastic substrate for cyclic stretch stimulation. A 0.1-mm-thick silicone rubber membrane (23 × 44 mm) was glued to the bottom of a 10-mm-thick rectangular silicone rubber frame (23 × 44 mm and 20 × 20 mm, outside and inside dimensions, respectively) to obtain a stretch chamber. The fibroblasts were seeded at a density of 100 cells/mm onto the silicone membrane coated with fibronectin (50 μg/mL) and precultured statically for 24 hours.

After an additional 12 hours of static culture, within an area of approximately 4 mm^2, cell morphology and orientation were confirmed using a phase contrast microscope, and cells were classified into two groups: one exhibiting no specific orientation (**Figure 1(A)**: the control cells with random orientation (CON)), and another where cell-cell contacts resulted in relatively elongated cell shapes oriented in a particular direction (**Figure 1(B)**: the control cells with natural orientation (CON-OR)).

Furthermore, as another group of cells, the cells were subjected to a simple uniaxial cyclic stretch at a strain amplitude of 10% and a frequency of 0.5 Hz for 12 hours using a cell stretching apparatus (ShellPa, Menicon, Japan) in CO_2 incubator (37°C, 5% CO_2 and 95% air). After the stretching, the cells elongated almost perpendicular to the stretching direction. Their actin cytoskeleton formed thick bundles of stress fibers with remarkable alignment (**Figure 1(C)**: cells with remarkable orientation induced by cyclic stretch stimulation (CSS-OR)).

In addition to the cell samples used in the wound healing experiment, separate cell samples of the three groups were prepared. These were fixed and permea-

bilized with phosphate-buffered saline (PBS(-), Nissui) containing 3.7% formaldehyde for 10 min and PBS(-) containing 0.5% Triton X-100 (ICN Biomedicals) for 5 min, respectively, and then stained with 200 nM Alexa Fluor 488-conjugated phalloidin (Molecular Probes) for 60 min and stained with 3 μM Hoechst 33342 (Invitrogen) for 30 min to visualize the actin cytoskeleton and intranuclear DNA, respectively, for detailed observation.

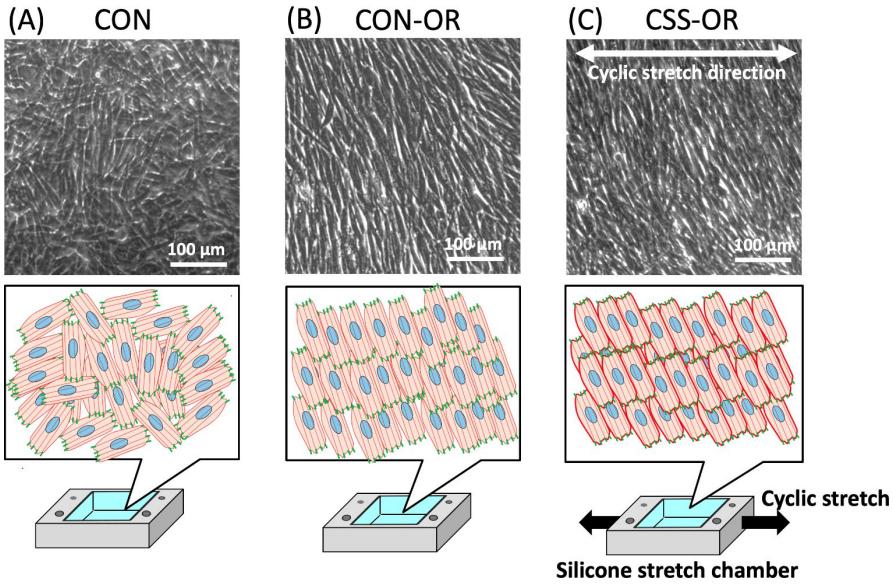

Figure 1. Typical phase contrast images of the control skin fibroblasts with random orientation (A: CON), the control fibroblasts with natural orientation (B: CON-OR), and fibroblasts with remarkable orientation induced by cyclic stretch stimulation for 24 hours (C: CSS-OR).

2.3. Cell Tissue Wounding with Laser Abrasion

To prepare wound healing models and observe wound closure processes, we used a laser ablation system developed in our laboratory [9]-[11], that incorporates a 355-nm-wavelength nanosecond pulsed laser unit (FTSS355-Q1, CryLas), a motorized XYZ stage (ProScan, Prior), a digital CMOS camera (ORCA-Fusion, C14440, Hamamatsu Photonics), and a light-emitting diode (LED) light source (X-Cite XLED1, Olympus) into an inverted fluorescent microscope (IX71, Olympus) (**Figure 2(A)**). The specimen cell tissues cultured on the silicone stretch chambers were set on a compact CO_2 incubator for microscope (Stage top incubator, Tokai Hit, Japan) to maintain the culture conditions (37˚C, 5% CO_2 and 95% air). The laser pulse frequency was set to 5000 Hz and the laser power to approximately 1.3 mW. The laser beam was focused onto the cells through a 20× objective lens (LCPLFLN, NA = 0.45, Olympus). Then, the motorized stage was then moved in the X direction, and the cell tissue was cut by irradiating it with the laser twice in a back-and-forth motion. The created linear wound area was approximately 100 μm width in the three groups of specimens prepared in the previous section (**Figure 2(B)**). Although nanosecond pulsed laser used in this

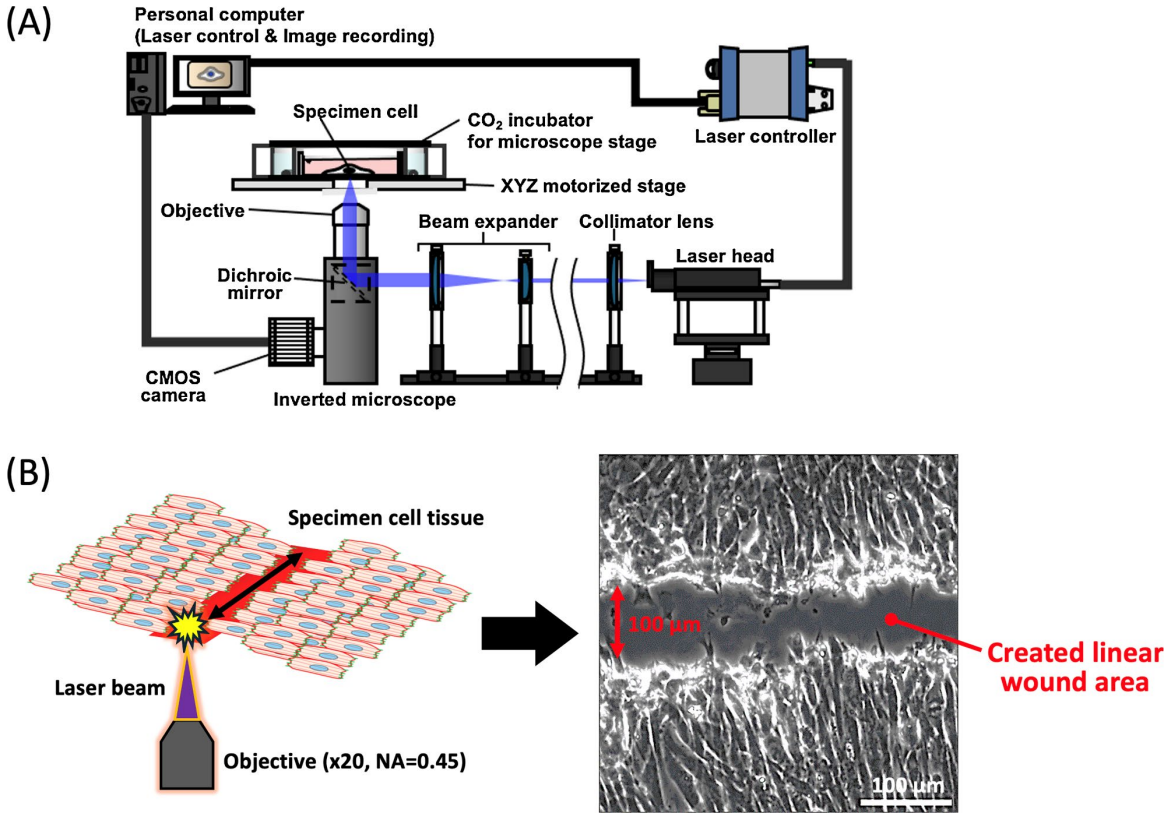

Figure 2. Schematic diagram of a laboratory-built laser ablation system including a pulsed laser for fabrication of linear wound (A). Cell tissue was cut by laser irradiating it twice in a back-and-forth motion, and the fabricated linear wound area was approximately 100 μm width (B).

study might cause necrosis in adjacent cells, the initial behavior of cells immediately after wounding was similar to that observed in conventional mechanical scraping experiments. To investigate how cell orientation affects wound-healing cell migration, linear wounds were created perpendicular to the direction of cell orientation for both the CON-OR group and the CSS-OR group. To analyze in detail the cell migration of wound closure processes, fluorescence images of intranuclear 53BP1 were used to track individual cell migration during wound healing.

2.4. Observation and Analysis of Wound Healing Processes

Before and after wounding, the time-lapse phase-contrast images of cells and the fluorescent images of the nuclei were captured. To measure changes in the area of laser-induced wounds, the phase-contrast images were imported into image analysis software (ImageJ, NIH). Then, a "Sharpen filter" was applied to the original images to enhance brightness variations, and the "Find edge" filter was used to extract contours, clearly defining the boundaries between wounds and cells. The images were then binarized, and only the wound area was selected for measurement (**Figure 3(A)**). The wound closure rate *WCR* was calculated based on the initial wound area using following equation.

$$WCR(t) = \frac{A(0) - A(t)}{A(0)} \times 100 \quad (1)$$

where, $A(0)$ and $A(t)$ are the initial wound area and the wound area at time t, respectively.

To analyze individual cell movements during the wound healing processes, the "TrackMate" plugin for ImageJ was used to obtain the center-of-mass coordinates of cell nuclei from fluorescence images of cell nuclei obtained during time-lapse observation. The initial x and y coordinates of the nuclei at the start of imaging were set as the origin, and cell migration direction was defined as the direction approximated by a straight line along the trajectory of the cell nucleus (Figure 3(B)). The sum of the nuclear displacement every 10 minutes was calculated to determine the total cell migration distance, and divided by the time to obtain the averaged cell migration speed S (μm/h). The cell migration direction θ was also assessed using a straight line along the trajectory of the cell nucleus (Figure 3(B), Right).

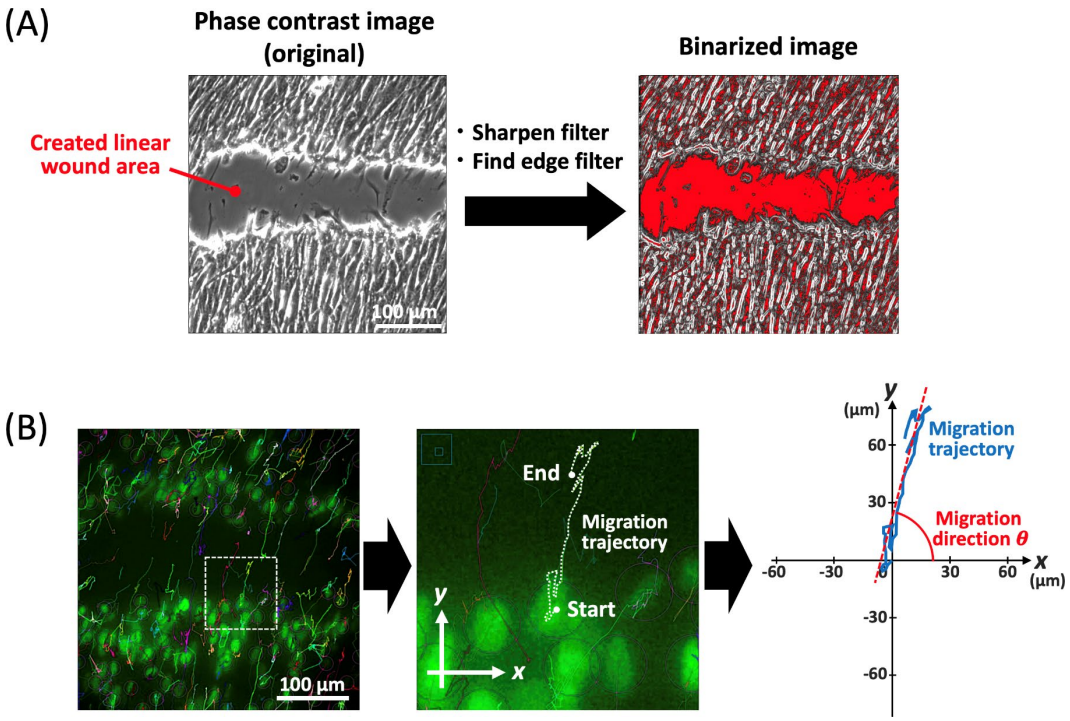

Figure 3. Procedures for analyzing the wound area of cellular tissue (A) and analyzing individual cell migration (B). The phase-contrast images of cells were processed with image filters to enhance the contours of the wound area, converting them into binary images (A). The migration distance and migration direction of cells were analyzed based on the trajectory of the center-of-mass of fluorescently labeled cell nuclei (B).

2.5. Statistical Analysis

Data are expressed as means ± standard deviation (SD). Statistical significance was assessed using Student's paired and unpaired t-test with the statistical analysis program MEPHAS (https://alain003.phs.osaka-u.ac.jp/mephas/index_jp.html). A significance level of $P < 0.05$ and $P < 0.01$ was used for all analyses.

3. Results and Discussion

Figure 4 shows representative images of wound closure behavior and time-course changes in wound area ($A(t)$) and wound closure rate ($WCR(t)$) for the three groups of skin fibroblasts. In all three groups, the wound gradually closed through cell migration (Figure 4). However, the wound in the CON-OR group was completely closed 10 hours after wounding (Figure 4(B)), while the wounds in the other two groups appeared incompletely closed (Figure 4(A) and Figure 4(C)).

Quantitative analysis of $A(t)$ and $WCR(t)$ revealed that the wound expanded further after injury in the CON group. Although wound closure behavior gradually occurred after 100 min, $A(t)$ remained almost unchanged from the initial value (Figure 4(D) and Figure 4(E), CON). In contrast, in the CON-OR group, the wound initially increased at 60 min after wounding but then rapidly closed, achieving complete closure by 340 min (Figure 4(D) and Figure 4(E), CON-OR). The CSS-OR group differed from the other two groups. A(t) and WCR(t) showed little change until 200 minutes after wounding, followed by an increase in wound closure behavior (Figure 4(D) and Figure 4(E), CSS-OR).

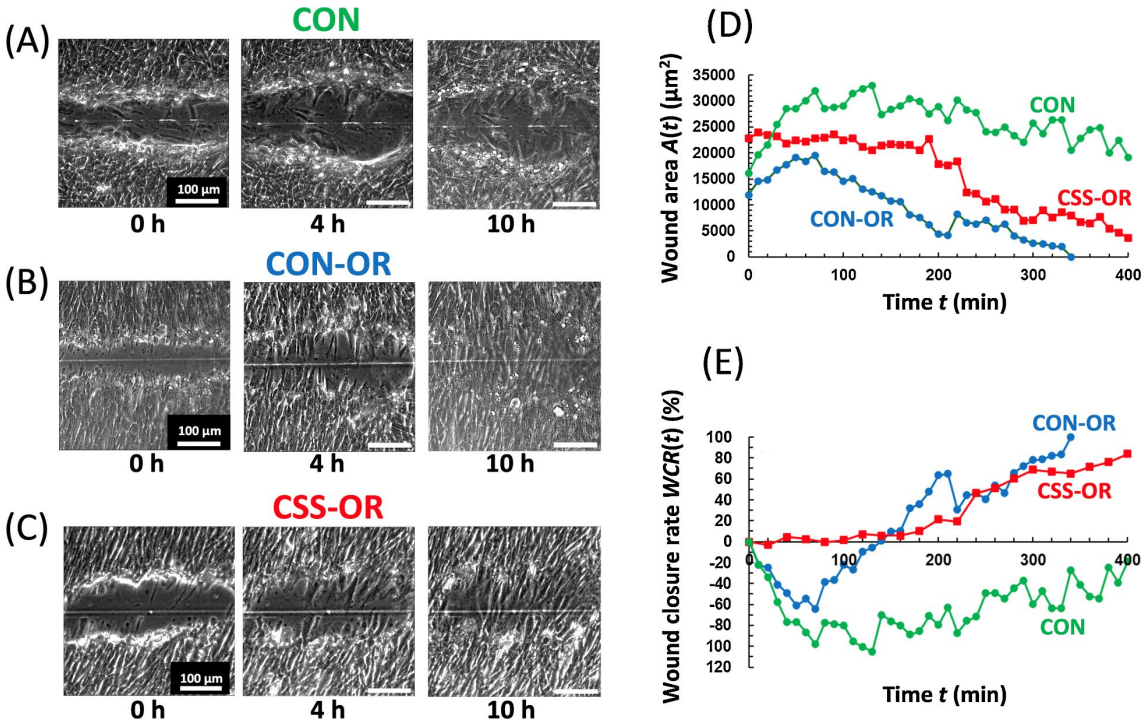

Figure 4. Examples of the time course images of the wound closure behavior of fibroblast monolayer with random orientation ((A): CON), with natural orientation ((B): CON-OR), and with remarkable orientation induced by cyclic stretch stimulation for 24 hours ((C): CSS-OR). The wound closure area $A(t)$ (D) and the wound closure rate $WCR(t)$ (E) was measured from the image stacks of A-C.

Figure 5 shows fluorescent images of cell nuclei (A, C, E) and nuclear migration trajectories (B, D, F) during wound closure behavior in each group, along with cell migration speed S(G) quantified from these data. The cell migration was quite random in the CON group (Figure 5(B)). In contrast, cells preferentially migrated

toward the wound closure direction in both CON-OR (Figure 5(D)) and CSS-OR (Figure 5(F)), following their initial orientation. Especially, the variation of migration direction was significantly smaller in CON-OR ($\theta = 69.4 \pm 12.6$ deg.) than in CON ($\theta = 38.2 \pm 21.2$ deg.) and CSS-OR ($\theta = 69.5 \pm 35.1$ deg.), resulting in the highest migration speed S for the CON-OR (Figure 5(G), blue bar). These results suggest that CON-OR cells exhibited the most efficient migration for wound closure, whereas CSS-OR cells, despite exhibiting similar orientation as CON-OR, demonstrated restricted initial cell migration toward wound closure.

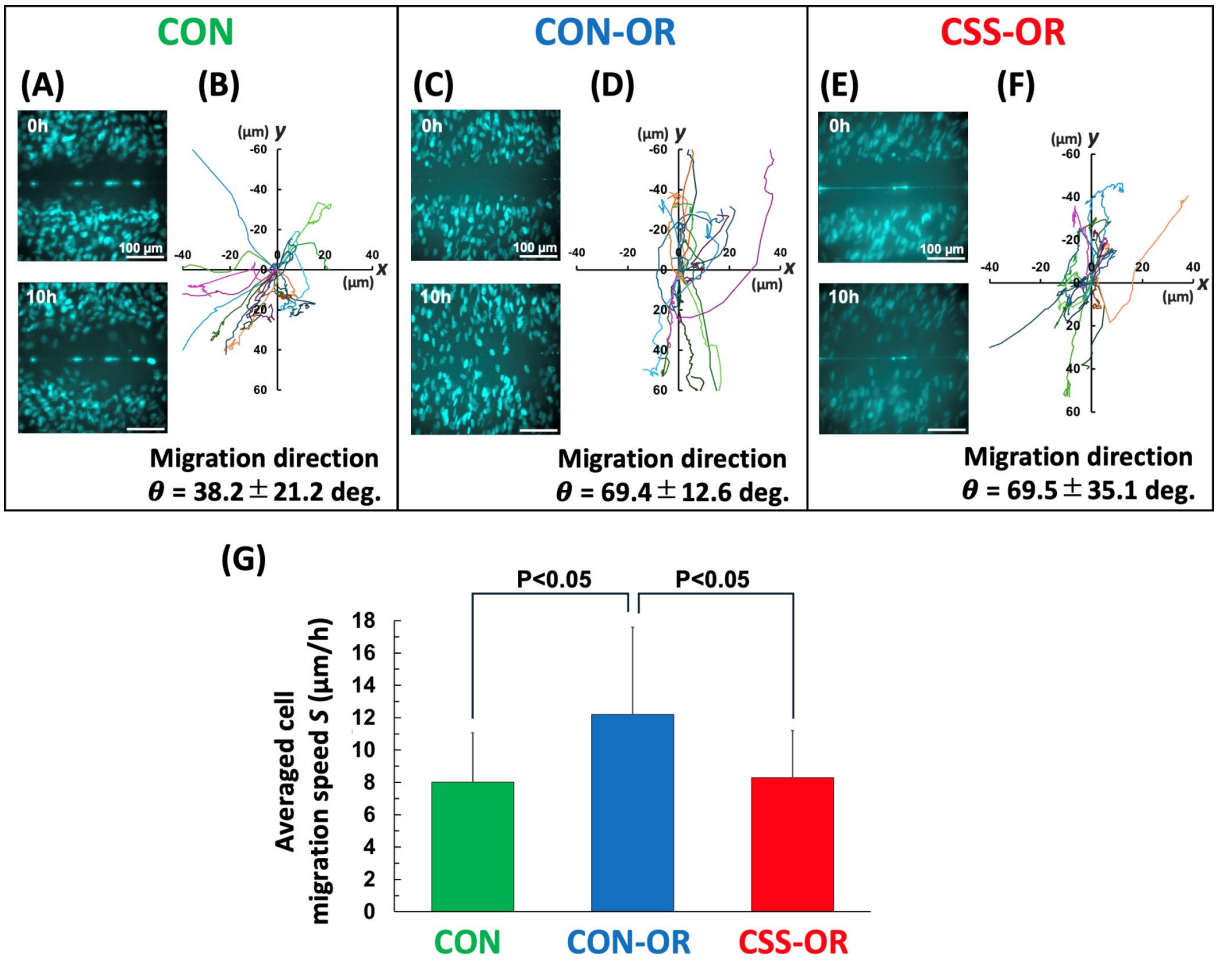

Figure 5. Examples of fluorescence images of the fibroblast nuclei ((A), (C), (E)) and the migration trajectory ((B), (D), (F)) of the three groups during the wound closure behavior. The averaged cell migration speed S (G) was quantified from these the migration trajectories (Mean + SD. n=20 cells were analyzed in each group).

Figure 6 shows detailed images of the actin cytoskeleton in the three cell groups. Before wound formation, the actin cytoskeleton in the CON group ran in various directions, exhibiting numerous fine, indistinct mesh-like structures (Figure 6(A)). In the CON-OR group, while fine, sparse actin cytoskeletons were also prevalent like in the CON group, they tended to be oriented toward the direction of wound closure (Figure 6(B)). In both groups, slight gaps were visible between cells, suggesting loosened intercellular adhesion. In contrast, the CSS-OR group exhibited

thick bundles of actin cytoskeletons oriented throughout the entire space of cells (Figure 6(C)). It has been reported that mechanical stimulation promotes the development of the actin cytoskeleton, increasing cellular traction forces and promoting the development of focal adhesions [12] [13]. Thus, the development of the actin cytoskeleton in the CSS-OR group might have strengthened cell-matrix adhesion, thereby suppressing the migration of the cells themselves immediately after wound formation.

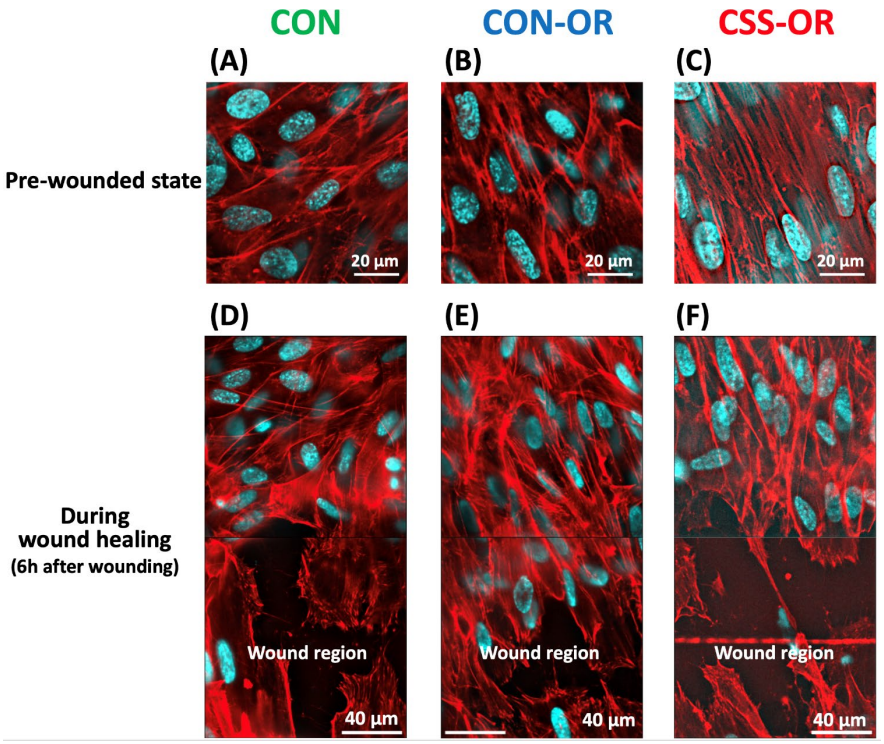

Figure 6. Fluorescence images of actin cytoskeleton (red) and nuclei (cyan) of fibroblast monolayer with random orientation (CON), with natural orientation (CON-OR), and with remarkable orientation induced by cyclic stretch stimulation for 24 hours (CSS-OR) at the pre-wounded state (A-C) and the wound healing migtration state (D–F). The panels below were created by combining two fluorescence images.

Finaly, the three cell tissue groups during wound healing were fixed, stained, and observed in detail. The actin cytoskeleton in the CON and CON-OR groups showed no significant changes from the pre-wound state (compare Figure 6(A) and Figure 6(D); compare Figure 6(B) and Figure 6(E)). In contrast, in the CSS-OR group, the thick bundle of actin cytoskeleton observed throughout the cells significantly remodeled to accumulate at the cell periphery where cells were attached to each other (compare Figure 6(C) and Figure 6(F)). This type of actin remodeling likely strengthened cell-cell adhesion, creating an effect in which the actin cytoskeleton of neighboring cells might pull back cells attempting to migrate during wound healing, thereby suppressing the wound-healing migration of neighboring cells. Furthermore, actin cytoskeletal remodeling in response to mechanical stimulation has been reported to begin three hours after the mechanical stim-

ulation [14]. This aligns well with the delayed cell migration observed in the CSS-OR group during the wound healing process in this study.

In summary, it has been demonstrated that cyclic stretch stimulation of cellular tissue promotes cell alignment and the maturation of actin stress fibers. This process may enhance cell-matrix adhesion and strengthen cell-cell adhesion, thereby stabilising the overall strength of the tissue. However, this stimulation conversely inhibits the wound-healing migration of cells.

Acknowledgements

This work was supported in part by a Grant-in-Aid from the Ministry of Education, Culture, Sports, Science, and Technology, Japan (nos. 24K03246, 23K25998, and 25K22900); the Naito foundation, Japan; the Hagiwara foundation, Japan; the Takeda Science Foundation, Japan.

Conflicts of Interest

The authors declare no conflicts of interest regarding the publication of this paper.

References

[1] Zou, M.L., Teng, Y.Y., Wu, J.J., Liu, S.Y., *et al.* (2021) Fibroblasts: Heterogeneous Cells with Potential in Regenerative Therapy for Scarless Wound Healing. *Frontiers in Cell and Developmental Biology*, **9**, Article 713605. https://doi.org/10.3389/fcell.2021.713605

[2] Mohd Razali, N.A., Lin, W., Norzain, N.A. and Yu, Z. (2021) Controlling Cell Elongation and Orientation by Using Microstructural Nanofibre Scaffolds for Accelerating Tissue Regeneration. *Materials Science and Engineering: C*, **128**, Article 112321. https://doi.org/10.1016/j.msec.2021.112321

[3] Kanchanawong, P., Shtengel, G., Pasapera, A.M., Ramko, E.B., Davidson, M.W., Hess, H.F., *et al.* (2010) Nanoscale Architecture of Integrin-Based Cell Adhesions. *Nature*, **468**, 580-584. https://doi.org/10.1038/nature09621

[4] Sneider, A., Hah, J., Wirtz, D. and Kim, D. (2019) Recapitulation of Molecular Regulators of Nuclear Motion during Cell Migration. *Cell Adhesion & Migration*, **13**, 50-62. https://doi.org/10.1080/19336918.2018.1506654

[5] Tanaka, T., Naruse, K. and Sokabe, M. (2005) Effects of Mechanical Stresses on the Migrating Behavior of Endothelial Cells. In: *Biomechanics at Micro- and Nanoscale Levels*, World Scientific, 75-87. https://doi.org/10.1142/9789812569301_0007

[6] Crosby, L.M., Luellen, C., Zhang, Z., Tague, L.L., Sinclair, S.E. and Waters, C.M. (2011) Balance of Life and Death in Alveolar Epithelial Type II Cells: Proliferation, Apoptosis, and the Effects of Cyclic Stretch on Wound Healing. *American Journal of Physiology-Lung Cellular and Molecular Physiology*, **301**, L536-L546. https://doi.org/10.1152/ajplung.00371.2010

[7] Nagayama, K., Suzuki, Y. and Fujiwara, D. (2019) Directional Dependence of Cyclic Stretch-Induced Cell Migration in Wound Healing Process of Monolayer Cells. *Advanced Biomedical Engineering*, **8**, 163-169. https://doi.org/10.14326/abe.8.163

[8] Kawamura, K., Suzuki, K. and Mitsutake, N. (2021) Technical Report: A Simple and Robust Real-Time Quantitative PCR Method for the Detection of Radiation-Induced

Multiple Exon Deletions of the Human HPRT Gene. *Radiation Research*, **199**, 83-88. https://doi.org/10.1667/rade-21-00047.1

[9] Nagayama, K., Yahiro, Y. and Matsumoto, T. (2011) Stress Fibers Stabilize the Position of Intranuclear DNA through Mechanical Connection with the Nucleus in Vascular Smooth Muscle Cells. *FEBS Letters*, **585**, 3992-3997. https://doi.org/10.1016/j.febslet.2011.11.006

[10] Nagayama, K., Nogami, K., Sugano, S. and Nakazawa, M. (2024) Dedifferentiation-And Aging-Induced Loss of Mechanical Contractility and Polarity in Vascular Smooth Muscle Cells: Heterogeneous Changes in Macroscopic and Microscopic Behavior of Cells in Serial Passage Culture. *Journal of the Mechanical Behavior of Biomedical Materials*, **160**, Article 106744. https://doi.org/10.1016/j.jmbbm.2024.106744

[11] Kambe, C. and Nagayama, K. (2025) Laser Nanodissection for Intracellular Actin Stress Fibers and Analysis of the Severed Fiber Retraction and Regeneration Behavior. *Transactions of the JSME* (*in Japanese*), **91**, Article 24-00271. https://doi.org/10.1299/transjsme.24-00271

[12] Na, S., Trache, A., Trzeciakowski, J., Sun, Z., Meininger, G.A. and Humphrey, J.D. (2008) Time-Dependent Changes in Smooth Muscle Cell Stiffness and Focal Adhesion Area in Response to Cyclic Equibiaxial Stretch. *Annals of Biomedical Engineering*, **36**, 369-380. https://doi.org/10.1007/s10439-008-9438-7

[13] Nagayama, K. and Fukuei, T. (2020) Cyclic Stretch-Induced Mechanical Stress to the Cell Nucleus Inhibits Ultraviolet Radiation-Induced DNA Damage. *Biomechanics and Modeling in Mechanobiology*, **19**, 493-504. https://doi.org/10.1007/s10237-019-01224-3

[14] Nagayama, K., Kimura, Y., Makino, N. and Matsumoto, T. (2012) Strain Waveform Dependence of Stress Fiber Reorientation in Cyclically Stretched Osteoblastic Cells: Effects of Viscoelastic Compression of Stress Fibers. *American Journal of Physiology-Cell Physiology*, **302**, C1469-C1478. https://doi.org/10.1152/ajpcell.00155.2011